Implementation of Rapid Prototyping Tools for Power Loss and Cost Minimization of DC-DC Converters

Authors:

Amruta V. Kulkarni, Weiqiang Chen, Ali M. Bazzi

Date Submitted: 2019-01-07

Keywords: design optimization, user interface, user centered design, DC-DC converters, design methodology, rapid prototyping

Abstract:

In this paper, power loss and cost models of power electronic converters based on converter ratings and datasheet information are presented. These models aid in creating rapid prototypes which facilitate the component selection process. Through rapid prototyping, users can estimate power loss and cost which are essential in design decisions. The proposed approach treats main power electronic components of a converter as building blocks that can be arranged to obtain multiple topologies to facilitate rapid prototyping. In order to get system-level power loss and cost models, two processes are implemented. The first process automatically provides minimum power loss or cost estimates and identifies components for specific applications and ratings; the second process estimates power losses and costs of each component of interest as well as the whole system. Two examples are used to illustrate the proposed approaches—boost and buck converters in continuous conduction mode. Achieved cost and loss estimates are over 93% accurate when compared to measured losses and real cost data. This research presents derivations of the proposed models, experimental validation of the models and demonstration of a user friendly interface that integrates all the models. Tools presented in this paper are expected to be very useful for practicing engineers, designers, and researchers, and are flexible and adaptable with changing or new technologies and varying component prices.

Record Type: Published Article

Submitted To: LAPSE (Living Archive for Process Systems Engineering)

Citation (overall record, always the latest version):	LAPSE:2019.0023
Citation (this specific file, latest version):	LAPSE:2019.0023-1
Citation (this specific file, this version):	LAPSE:2019.0023-1v1

DOI of Published Version: https://doi.org/10.3390/en9070509

energies

MDPI

Article

Implementation of Rapid Prototyping Tools for Power Loss and Cost Minimization of DC-DC Converters

Amruta V. Kulkarni, Weiqiang Chen * and Ali M. Bazzi

Department of Electrical and Computer Engineering, University of Connecticut, Storrs, CT 06269, USA; kulkarni.amruta1@gmail.com (A.V.K.); bazzi@uconn.edu (A.M.B.)

* Correspondence: weiqiang.chen@uconn.edu; Tel.: +1-860-771-8222

Academic Editor: Gabriele Grandi

Received: 30 March 2016; Accepted: 20 June 2016; Published: 1 July 2016

Abstract: In this paper, power loss and cost models of power electronic converters based on converter ratings and datasheet information are presented. These models aid in creating rapid prototypes which facilitate the component selection process. Through rapid prototyping, users can estimate power loss and cost which are essential in design decisions. The proposed approach treats main power electronic components of a converter as building blocks that can be arranged to obtain multiple topologies to facilitate rapid prototyping. In order to get system-level power loss and cost models, two processes are implemented. The first process automatically provides minimum power loss or cost estimates and identifies components for specific applications and ratings; the second process estimates power losses and costs of each component of interest as well as the whole system. Two examples are used to illustrate the proposed approaches—boost and buck converters in continuous conduction mode. Achieved cost and loss estimates are over 93% accurate when compared to measured losses and real cost data. This research presents derivations of the proposed models, experimental validation of the models and demonstration of a user friendly interface that integrates all the models. Tools presented in this paper are expected to be very useful for practicing engineers, designers, and researchers, and are flexible and adaptable with changing or new technologies and varying component prices.

Keywords: rapid prototyping; design methodology; DC-DC converters; user centered design; user interface; design optimization

1. Introduction

1.1. Overview

As dependence on electronic appliances, digital products and computer systems in both industrial and household applications grows, the demand for power electronic converters is increasing. DC-DC converters continue to grow in popularity in all major electronics applications. Given the high demand for these converters, engineers are faced with a major challenge to design them in a very short period of time while still ensuring competitive cost. Rapid prototyping tools for converter development help solve this constraint and thus are of interest as both time- and cost-saving methods.

Existing literature indicates significant research related to power loss estimation of various power electronic components. Loss estimation, for example, is used in [1] to analyze how power loss can be redistributed in a power converter using a modulation technique. Another reason for the need for power loss estimation is when evaluating the effect of different material on device power losses, e.g., [2,3]. In other applications, e.g., [4], power loss estimation is central in evaluating the usability of a power electronic converter, and power loss is used as a metric when comparing various converters. Since temperature rise in semiconductors and other power electronic devices is mainly caused by power losses, power losses have also been used for thermal analysis and modeling of power electronic

systems, e.g., [5,6]. Therefore, power loss estimation is essential for new material, device, and converter evaluation, in addition to comparing various converters and designs where efficiency is a major figure of merit. Modeling of power electronic converters can be improved by loss and cost estimation, such as distributed power converters in a standalone DC microgrid [7], or DC microgrids for electric vehicle charging stations [8]. Also, essential application which relies on power converter topology can benefit from loss and cost estimation, like PFC converters for plug-in-hybrid electric vehicles [9], and novel bidirectional DC/DC converter topologies [10].

Several techniques have been implemented to find out power loss or cost models of specific components. A majority of this research has focused on selecting components for power electronic converters, e.g., [11]. Extensive research has been conducted for finding specific losses in semiconductors and magnetic components, e.g., [12]. Power loss estimation in semiconductors has also been extensively studied, e.g., [6,13] where power losses are correlated with temperature rise in the devices using thermal resistance datasheet values. Topology-specific power loss models also exist, which address specific component losses, e.g., power MOSFET losses in a buck converter [14], or system-level losses, e.g., boost converter [15]. Several methods to measure system-level power loss have also been proposed, e.g., [16,17]. Power losses in other parts of the converter, e.g., PCB losses [18–20] and gate drive losses [21], have been addressed but are only introduced in the Appendix A of this paper.

Cost consideration is the most important factor for industries which mass-produce power electronic converters, to achieve market success and competitiveness by reducing cost [22]. However, most existing literature mainly focuses on methods to predict costs of specific systems and avoids generalized cost models of power electronic devices and converters. For example, in [23] the cost models of a battery, inverter and converter were developed on the basis of power ratings of these sub-systems. Cost estimation and reduction techniques have been developed for a single component such as inductor or heat sink in [24]. Some cost models are also developed for switch-mode power supplies by considering component power losses, weight, manufacturing process and raw material cost fluctuations [25].

An important application of power loss and cost estimation is design optimization of power electronic converters. With a well-established power loss or cost model of various devices that can form the converter, an optimization problem can be established where the converter's power loss or cost are the figures of merit. Attempts for such analytical design approaches are [26], but mostly focus on power losses, especially semiconductor losses in [26]. Cost models and power loss models of specific devices which can be extended for integration in power electronic converters, have been presented in [27] but without converter design optimization.

Therefore, generalized power loss models of major power electronic devices, as well as cost models of these devices, have not been shown in the literature for ease of integration for any power converter topology. For example, textbook models such as those presented in [16,28–30], are presented in an introductory ay where they may not be easily integrated into any power converter topology. Research papers, on the other hand, present very specific models for devices or topologies but rarely provide a flexible model that can be integrated with different power converter topologies.

1.2. Proposed Approach and Contribution

This paper presents a building-block approach, as demonstrated in Figure 1, towards modeling power loss and the cost of power electronic converters. Power loss models are based on converter voltage, current, power, and frequency ratings and operating conditions along with basic datasheet information. Cost models are based on average prices related to component ratings obtained using an extensive market survey and surface-fitting tools. It is important to note that component technology and cost profiles change over time as a result of changes in material and manufacturing techniques and thus this paper intends to develop power loss and cost modeling methodologies that can evolve with time and changes in technology.

The paper focuses on the building-block approach of the modeling of power loss and the cost of power electronic converters to achieve minimum power loss and cost design instead of the model

construction of single component. The proposed method provides a new tool and effective way where assembles the circuit from parts to an entirety to evaluate the power loss and cost of an entire converter. The overall process used in rapid prototyping tools for cost and power loss models in optimization and component-specific modes as proposed here is illustrated in Figure 2. The target of the models is to minimize the estimation error when comparing actual component power loss and cost values with the measured power losses or actual cost. Their main advantage is the ability to evaluate a large number of possible component combinations and achieve almost instantaneous cost and loss estimates. Thus a large quantity component library is generated as the basement of the models and the web based program of the rapid prototyping tool ensures the component library is up to date along with the newest marketing price and technology. From customer perspective, once the converter topology is chosen and desired power loss and cost are typed into the GUI interfacing panel, the rapid prototyping tool is able to search, chose the appropriate component and assemble the converter rapidly to save the time of customer to search and evaluate the component. Also, the rapid prototyping tool is able to optimize the results to minimize the power loss and cost with the change of the custom parameters such as topology, total cost and power loss.

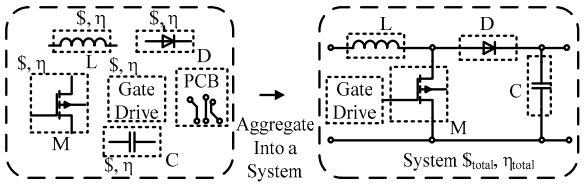

Figure 1. Example illustration on how to aggregate component level models into a system ($: Cost, η: Efficiency).

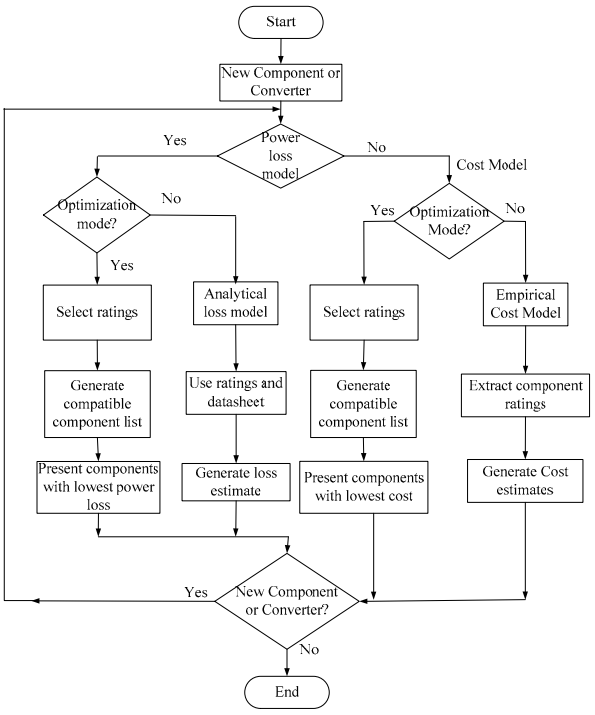

Figure 2. Procedure for the proposed rapid prototyping tools.

Rapid prototyping tools for DC-DC converters are of main interest here due to the converters' simplicity, wide range of their applications and since the methodology for developing models is of main interest rather than actual topologies.

The paper proceeds as follows: Section 2 shows generalized component-level power loss models. Section 3 discusses the application of generalized power loss models for several power electronic converters. Section 4 explains the concept behind cost model development and illustrates these models. Section 5 shows experimental results that validate the developed models. Section 6 explains rapid prototyping tools for model-based power loss minimization and presents tools for cost minimization. Section 7 concludes with the summary remarks and future work.

2. Generalized Component-Level Power Loss Models

Generalized power loss models of power electronic components are derived based on equivalent circuit models of each major component by considering component non-idealities and parasitic elements. The models presented here stem from existing models in textbooks and foundational research papers, e.g., [13,19,28–30] and others. Therefore, this Section is a summary of such models, while Section 3 presents these models when massaged for specific buck and boost converter topologies.

2.1. MOSFET Losses

In power electronic converters, MOSFETs operate as switching elements. Figure 3 shows a MOSFET model with its non-idealities.

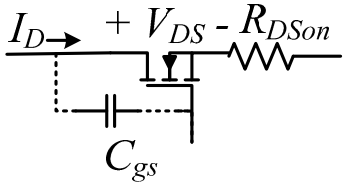

Figure 3. MOSFET model with non-idealities.

The MOSFET P_{CM} [28] is:

$$P_{CM} = R_{DSon} I_{Drms}^2 \tag{1}$$

where I_D is represented as shown in Figure 4 when the MOSFET operates as a switch. I_{Drms} can be computed by $I_{Drms} = \sqrt{\frac{1}{T}\int_0^T \left(\frac{\Delta i}{DT}t + I_{Lavg} - \frac{1}{2}\Delta i\right)^2 dt} = \sqrt{\frac{1}{3}\Delta i^2 D + (I_{Lavg} - \frac{1}{2}\Delta i)\Delta i D + (I_{Lavg} - \frac{1}{2}\Delta i)^2 D}$.

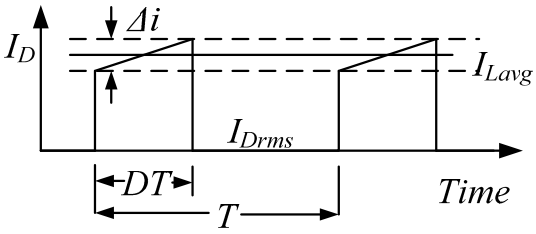

Figure 4. MOSFET drain current.

Switching losses of MOSFETs are mainly divided into two parts, $P_{ON(M)}$ and $P_{OFF(M)}$. Because only steady state efficiency is concerned, voltage overshoot and diode reverse recovery effect won't be considered. The total switching loss P_{SW} is thus [31]:

$$P_{SW} = P_{ON(\mathrm{M})} + P_{OFF(\mathrm{M})} \tag{2}$$

where for a fixed f_{sw}:

$$P_{ON(M)} = \frac{1}{2} V_{DS} I_{Don} (t_r + t_{d(on)}) f_{sw} \tag{3}$$

$$P_{OFF(M)} = \frac{1}{2} V_{DS} I_{Doff} (t_f + t_{d(off)}) f_{sw} \quad (4)$$

The gate loss P_G is usually observed at C_{gs} [17]:

$$P_G = Q_{gs} V_{Supply} f_{sw} \quad (5)$$

Thus, total power losses in a MOSFET are:

$$P_{loss(\text{MOSFET})} = P_{CM} + P_{SW} + P_G \quad (6)$$

2.2. Diode Losses

Diodes in power electronic converters act as rectifiers and uncontrolled switches. Figure 5 shows a diode model with its non-idealities.

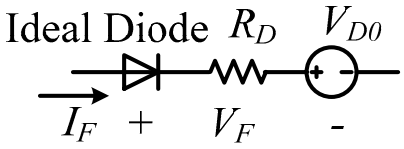

Figure 5. Diode model with non-idealities.

The diode conduction loss P_{CD} is modeled as:

$$P_{CD} = V_{D0}(1 - D) I_{Favg} + R_D (1 - D) I_{Frms}^2 \quad (7)$$

where typical values of V_{D0} and R_D are:

$$V_{D0} = V_{D\max} / V_{Dtyp} \quad (8)$$

$$R_D = \Delta V_F / \Delta I_F \quad (9)$$

There are two switching losses of a diode—turn-on loss and turn-off loss. The turn-on loss is usually ignored because the diode starts conducting from an off-state. P_{SWD} is thus [6]:

$$P_{SWD} = \frac{1}{2} Q_{rr} V_{rr} f_{sw} \quad (10)$$

and the total diode power loss is:

$$P_{loss(Diode)} = P_{CD} + P_{SWD} \quad (11)$$

2.3. Inductor Losses

An inductor stores energy in its magnetic field. Figure 6 shows an inductor with non-idealities and Figure 7 shows a typical inductor current waveform in a DC-DC converter.

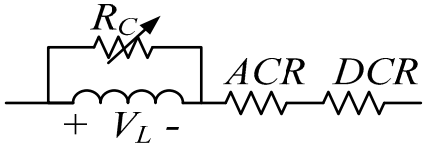

Figure 6. Inductor model with non-idealities.

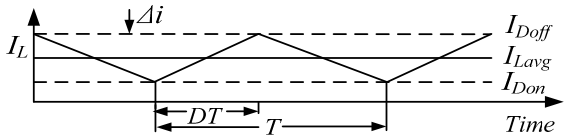

Figure 7. Inductor current waveform.

The core loss P_{CORE} is usually obtained by the Steinmetz equation [16,32] to be:

$$P_{CORE} = K_1 f^x B^y V_e \tag{12}$$

Note that modified Steinmetz equations are also common for core loss estimation, but if core loss coefficients are not supplied in a datasheet, a constant R_C can be used and P_{CORE} is estimated as:

$$P_{CORE} \approx \frac{V_L^2}{R_C} \tag{13}$$

The Steinmetz equation is used as an example, but the methodology is intended to support other forms of loss models. This is clear by using either Equation (12) or Equation (13) and can extend to more detailed models. Resistive losses can also be estimated as shown in [16,32], *DCR* and *ACR* are provided by datasheets or manufacturers:

$$P_{DCR} = I_{Lavg}^2 DCR \tag{14}$$

$$P_{ACR} = I_{Lrms}^2 ACR \tag{15}$$

Total power loss of an inductor is thus:

$$P_{loss(Inductor)} = P_{CORE} + P_{DCR} + P_{ACR} \tag{16}$$

2.4. Capacitor Losses

Capacitors are major storage elements in power electronic converters and their typical non-idealities are shown in Figure 8.

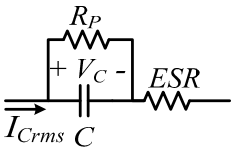

Figure 8. Capacitor model with non-idealities.

Two major power losses in the capacitor are those in its AC and DC resistances [33]. P_{ac} is:

$$P_{ac} = I_{Crms}^2 ESR \tag{17}$$

while P_{dc} is:

$$P_{dc} = \frac{V_C^2}{R_P} \tag{18}$$

Total power loss of the capacitor is thus:

$$P_{loss(Capacitor)} = P_{ac} + P_{dc} \tag{19}$$

P_{dc} is small as compared to P_{ac} as capacitors are mainly used to pass current ripple, thus P_{dc} it is frequently ignored.

3. Power Loss Models for Several Converters

Equations explained in the previous section are common in the literature, but are rarely presented for specific converter topologies. In this section power loss models for boost and buck converter in continuous conduction mode (CCM) and flyback converter in discontinuous conduction mode (DCM) are explained in detail. These converters are used as examples due to their common use in any applications and their simple construction and analysis. All generalized equations are reformulated in terms of input and output parameters and datasheet information.

3.1. Boost Converter in CCM

A typical non-ideal boost converter is shown in Figure 9 followed by derivations for power losses in main boost converter components operating in CCM.

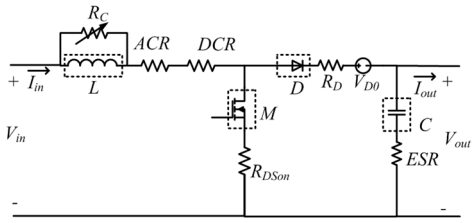

Figure 9. Boost converter with its non-idealities.

3.1.1. MOSFET Losses

P_{CM} is obtained from Equation (1) and can be estimated [34] as:

$$P_{CM} = R_{DSon} D \left[I_{in}^2 + \frac{\Delta i^2}{12} \right] \tag{20}$$

To calculate P_{SW}, I_{Don} and I_{Doff} can be obtained from Figure 7:

$$I_{Don} = I_{in} - \frac{\Delta i}{2} \tag{21}$$

$$I_{Doff} = I_{in} + \frac{\Delta i}{2} \tag{22}$$

$$V_{DS} = V_{in} \tag{23}$$

Thus, $P_{ON(M)}$ and $P_{OFF(M)}$ are calculated as:

$$P_{ON(\mathrm{M})} = \frac{1}{2} V_{in} \left(I_{in} - \frac{\Delta i}{2} \right) t_r f_{sw} \tag{24}$$

$$P_{OFF(\mathrm{M})} = \frac{1}{2} V_{in} \left(I_{in} + \frac{\Delta i}{2} \right) t_f f_{sw} \tag{25}$$

3.1.2. Diode Losses

P_{CD} and P_{SWD} are obtained using Equations (7) and (10) as:

$$P_{CD} = V_{D0}(1 - D) I_{in} + R_D (1 - D) I_{in}^2 \tag{26}$$

$$P_{SWD} = \frac{1}{2} Q_{rr} \left(V_{out} - V_{in} - I_{in} DCR \right) f_{sw} \tag{27}$$

3.1.3. Inductor Losses

P_{CORE}, P_{DCR} and P_{ACR} can be calculated as:

$$P_{CORE} \approx \frac{(V_{out} - V_{in} - I_{in}DCR - V_F)^2}{R_C} \tag{28}$$

$$P_{DCR} = I_{in}^2 DCR \tag{29}$$

$$P_{ACR} = \frac{\Delta i^2}{12} ACR \tag{30}$$

3.1.4. Capacitor Losses

$P_{loss(Capacitor)}$ is obtained using Equation (17) as:

$$P_{loss(Capacitor)} = \frac{\Delta i^2}{12} ESR \tag{31}$$

3.2. Buck Converter in CCM

A typical non-ideal buck converter is shown in Figure 10.

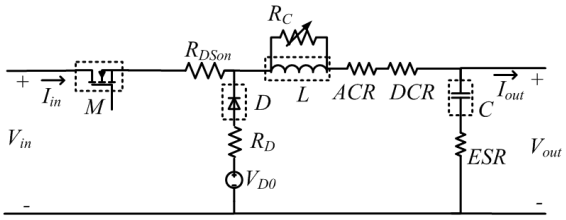

Figure 10. Buck converter topology for power loss model.

3.2.1. MOSFETs Losses

P_{CM} is obtained from Equation (1) and can be estimated [30] as:

$$P_{CM} = R_{DSon} D \left[I_{out}^2 + \frac{\Delta i^2}{12} \right] \tag{32}$$

To calculate P_{SW}, I_{Don} and I_{Doff} can be obtained from Figure 7 and V_{DS} as in Equation (23). Thus, P_{ON} and P_{OFF} are calculated as:

$$I_{Don} = I_{out} - \frac{\Delta i}{2} \tag{33}$$

$$I_{Doff} = I_{out} + \frac{\Delta i}{2} \tag{34}$$

$$P_{ON(\mathrm{M})} = \frac{1}{2} V_{in} \left(I_{out} - \frac{\Delta i}{2} \right) t_r f_{sw} \tag{35}$$

$$P_{OFF(\mathrm{M})} = \frac{1}{2} V_{in} \left(I_{out} + \frac{\Delta i}{2} \right) t_f f_{sw} \tag{36}$$

3.2.2. Diode Losses

P_{CD} and P_{SWD} are obtained by referring Equations (7) and (10) as:

$$P_{CD} = V_{D0}(1 - D) I_{out} + R_D (1 - D) I_{out}^2 \tag{37}$$

$$P_{SWD} = \frac{1}{2} Q_{rr} \left(V_{out} + I_{out} DCR \right) f_{sw} \tag{38}$$

3.2.3. Inductor Losses

P_{CORE}, P_{DCR} and P_{ACR} can be calculated as:

$$P_{CORE} \approx \frac{\left(V_{in} - V_{out} - I_{in} R_{DSon} - I_{out} DCR \right)^2}{R_C} \tag{39}$$

$$P_{DCR} = I_{out}^2 DCR \tag{40}$$

$$P_{ACR} = \frac{\Delta i^2}{12} ACR \tag{41}$$

3.2.4. Capacitor Losses

$P_{loss\ (Capacitor)}$ is obtained using Equation (17) as:

$$P_{loss(Capacitor)} = \frac{\Delta i^2}{12} ESR \tag{42}$$

3.3. Flyback Converter in DCM

Flyback converters are widely used in DCM. A non-ideal flyback converter in DCM is shown in the Figure 11. For the sake of illustration, the MOSFET switching period was considered as $T_{ON} + T_{OFF} = 0.8T_S$ as shown in Figure 12.

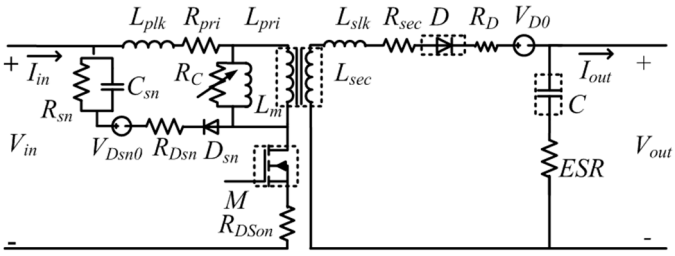

Figure 11. Flyback converter model with its non-idealities.

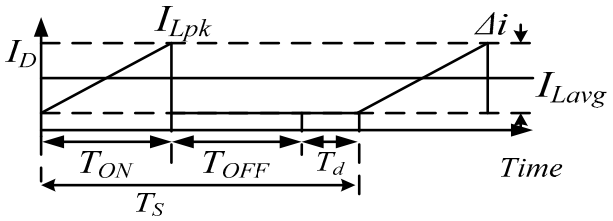

Figure 12. MOSFET switching waveform.

3.3.1. MOSFET Losses

$$T_{ON} = \frac{0.8 T_S \left(V_{out} + V_F \right)}{V_F} \tag{43}$$

$$V_{DS} = V_{in} + n V_{out} \tag{44}$$

P_{CM} in the flyback converter is described in [30,35] as:

$$P_{CM} = R_{DSon}\left(\frac{V_{in}}{(L_m + L_{pri})\, f_{sw}} D\sqrt{0.26\left(1 + \frac{V_{out}}{V_F}\right)}\right)^2 \tag{45}$$

For a flyback converter in DCM, I_{Don} is zero but I_{Doff} and P_{SW} are determined using [35,36] and Figure 13 as:

$$I_{Doff} = \frac{0.9V_{in}D}{2\,(L_m + L_{pri})\, f_{sw}} \tag{46}$$

$$P_{SW} = P_{OFF(\mathrm{M})} = (V_{in} + nV_{out})\left[\frac{0.9V_{in}D}{2\,(L_m + L_{pri})}\right]\frac{t_f}{2} \tag{47}$$

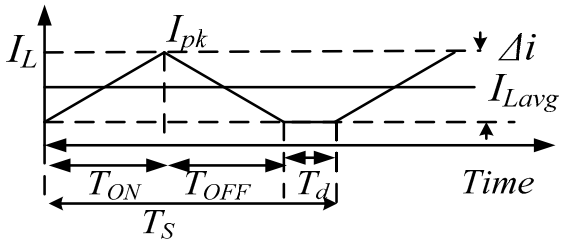

Figure 13. Inductor switching waveform.

3.3.2. Diode Losses

P_{CD} and P_{SWD} of the flyback diode are calculated as:

$$P_{CD} = V_{D0}(1 - D)I_{out} + R_D(1 - D)\left[\frac{0.52nV_{in}D}{(L_m + L_{pri})\, f_{sw}}\right]^2 \tag{48}$$

$$P_{SWD} = \frac{1}{2}Q_{rr}V_{out}f_{sw} \tag{49}$$

3.3.3. Flyback Coupled-Inductor/Transformer Lossses

P_{CORE} is given in [20,34,36] as:

$$P_{CORE} = K_{fe}B_{AC}^{\beta}A_C L_m \tag{50}$$

where:

$$B_{AC}^{\beta} = \frac{L_m \Delta i}{N_{pri}A_C} \tag{51}$$

Primary P_{Rpri} and secondary P_{Rsec} resistive power losses are calculated [21] as:

$$P_{Rpri} = \left(\frac{0.4V_{in}D}{(L_m + L_{pri})\, f_{sw}}\right)^2 R_{pri} \tag{52}$$

$$P_{R\mathrm{sec}} = \left(\frac{0.4nV_{in}D}{(L_m + L_{pri})\, f_{sw}}\right)^2 R_{\mathrm{sec}} \tag{53}$$

3.3.4. Capacitor Losses

Form Equation (17), $P_{loss(Capacitor)}$ is calculate as:

$$P_{loss(Capacitor)} = \left\{ \left[\frac{0.52nV_{in}D}{(L_m + L_{pri})\, f_{sw}} \right]^2 - I_{out}^2 \right\} ESR \tag{54}$$

3.3.5. Snubber Circuit Losses

The main components in the snubber branch are R_{sn}, C_{sn} and D_{sn}. R_{sn} and C_{sn} form a clamp unit. P_{clamp} is represented as [35]:

$$P_{clamp} = \frac{(V_{clamp})^2}{R_{sn}} = \frac{(0.9V_{DSBR} - V_{in})^2}{R_{sn}} \tag{55}$$

or:

$$P_{clamp} = \frac{1}{2} f_{sw} L_{pri} \Delta i^2 \left(1 + \frac{V_{in}}{0.9V_{DSBR} - 2V_{in}} \right) \tag{56}$$

Snubber diode conduction loss P_{CDsn} is obtained from Equation (7) as:

$$P_{CDsn} = V_{Dsn0}(1 - D)nI_{out} + R_{Dsn}(1 - D)nI_{Srms}^2 \tag{57}$$

while P_{SWDsn} is obtained as:

$$P_{SWDsn} = \frac{1}{2} Q_{rrsn} V_{in} f_{sw} \tag{58}$$

Total snubber circuit power loss is the summation of snubber diode power loss and power loss in the clamp unit. Therefore, all power loss equations for the three different converter examples are derived based on datasheet information and converter ratings. Results that validate the derived models are shown in Section 5 where experimental prototypes are used to measure the total loss in the converter.

4. Major Component Cost Models

A large database of cost information for multiple elements was compiled from common manufacturers' and suppliers' data. The two main sources of this data were Digikey [37] and Mouser Electronics [38], where searches were performed for MOSFETs, diodes, capacitors, and inductors of specific rating ranges. Search filters were applied to achieve such range limits, and the database is compiled and available for public use [39]. Since multiple options exist for different power, voltage, current, and/or device value rating (e.g., inductance and capacitance), the average cost for each component at a certain rating combination was found by considering these multiple options. This database was input to MATLAB to create interpolated graphs and find a mathematical relationship between cost and component ratings. Cost per quantity was also considered. The impact of time on cost is not considered due to availability of present prices only. Some other costs such as costs resulting from auxiliaries, heat sinks, fan/clod plates, etc are also not considered because they are beyond the scope of this work, where the focus is mainly on methodology.

4.1. MOSFETs

SiC and GaN type semiconductor cost is still varying rapidly due to continued production improvements, thus to demonstrate the methodology we focus on Si. To create a MOSFET cost model $Cost_M$, a large database was prepared using V_{DS}, I_D and cost. α_i coefficients are as listed in Table 1, but it should be noted that these coefficients vary across a certain range and the values shown are

selected to achieve the best fit for specific components used in Section 5. Figures 14 and 15 show the mathematical relationship for this database. $Cost_M$ is represented as:

$$Cost_M(V_{DS}, I_D) = \sum_{i=0}^{i=15} \alpha_i V_{DS}^{\beta_i} I_D^{\gamma_i} \tag{59}$$

Table 1. Coefficients for the MOSFET cost model equation.

Coefficient	Value	Range	β_i	γ_i
α_0	0.8091	$(-17.52, 19.14)$	0	0
α_1	0.01964	$(-0.06058, 0.09985)$	1	0
α_2	-0.1375	$(-2.465, 2.19)$	0	1
α_3	-3.497×10^{-5}	$(-0.0001393, 6.939 \times 10^{-5})$	2	0
α_4	-0.00323	$(-0.0106, 0.004137)$	1	1
α_5	0.01736	$(-0.08388, 0.1186)$	0	2
α_6	1.3×10^{-8}	$(-1.6 \times 10^{-6}, 1.6 \times 10^{-6})$	3	0
α_7	5.022×10^{-6}	$(-4.517 \times 10^{-6}, 1.456 \times 10^{-5})$	2	1
α_8	9.087×10^{-5}	$(-9.87 \times 10^{-5}, 0.0002804)$	1	2
α_9	-0.0005698	$(-0.002582, 0.001443)$	0	3
α_{10}	-8.033×10^{-8}	$(-2.976 \times 10^{-7}, 1.37 \times 10^{-7})$	2	2
α_{11}	-9.716×10^{-7}	$(-2.976 \times 10^{-6}, 1.032 \times 10^{-6})$	1	3
α_{12}	7.185×10^{-6}	$(-1.183 \times 10^{-5}, 2.62 \times 10^{-5})$	0	4
α_{13}	3.17×10^{-10}	$(-1.034 \times 10^{-9}, 1.668 \times 10^{-9})$	2	3
α_{14}	4×10^{-9}	$(-5.126 \times 10^{-9}, 1.313 \times 10^{-8})$	1	4
α_{15}	-3.103×10^{-8}	$(-1.006 \times 10^{-7}, 3.851 \times 10^{-8})$	0	5

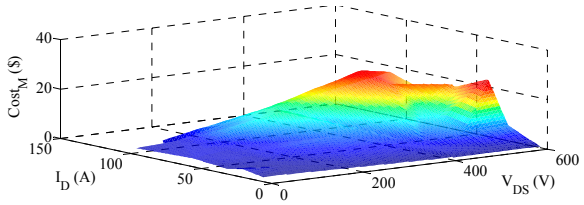

Figure 14. MOSFET cost model for one unit.

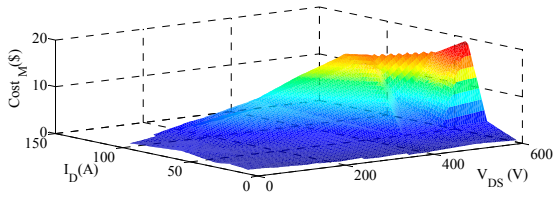

Figure 15. MOSFET cost model for 1000 units.

4.2. Diodes

A diode cost database was prepared using V_B, I_F and cost where Figures 16 and 17 show the interpolated cost surfaces while the mathematical model is shown in Equation (60) and its coefficients are shown in Table 2.

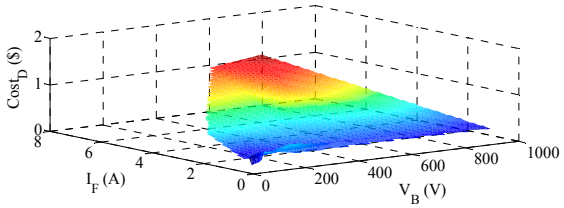

Figure 16. Diode cost model for one unit.

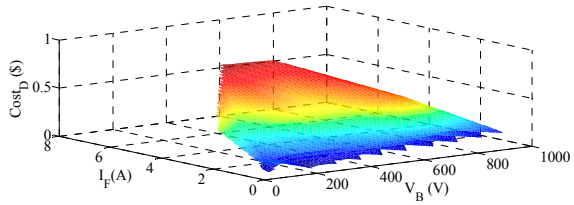

Figure 17. Diode cost model for 1000 units.

$$Cost_D(V_B, I_F) = \sum_{j=0}^{j=2} \delta_j V_B^{\theta_j} I_F^{\kappa_j} \tag{60}$$

Table 2. Coefficients for the diode cost model equation.

Coefficients	Value	Range	θ_j	κ_j
δ_0	0.22	(0.1, 0.3)	0	0
δ_1	7×10^5	$(-2.6 \times 10^{-4}, 1.2 \times 10^{-4})$	1	0
δ_2	0.1	(0.08, 0.13)	0	1

4.3. Inductors

Inductor cost data is compiled based on L, I_L and cost. Figures 18 and 19 show the interpolated cost surfaces while the mathematical model is shown in Equation (61) and its coefficients are where $x = 9.67$, $\mu = 61.64$, $\phi = -8.246$, $v = 4.495$, $\omega = -0.08658$.

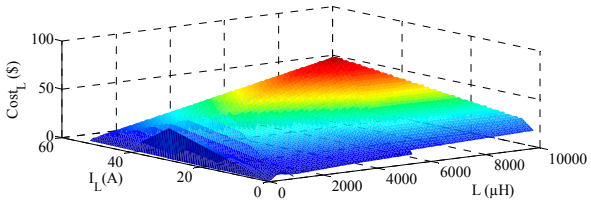

Figure 18. Inductor cost model for one unit.

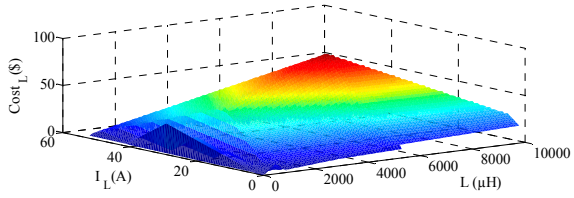

Figure 19. Inductor cost model for 1000 units.

$$Cost_L(L, I_L) = \chi + \mu \sin(v\pi L I_L) + \phi e^{-(\omega I_L)^2} \tag{61}$$

4.4. Capacitors

A capacitor cost ($Cost_C$) database for electrolytic capacitors was prepared using C, V_C and cost where Figures 20 and 21 show the interpolated cost surfaces while the model is shown in Equation (62) and its coefficients are shown in Table 3. Different material of capacitor will lead to different cost, but electrolytic capacitor is chosen as an example to illustrate the methodology:

$$Cost_C(C, V_C) = \sum_{z=0}^{z=8} \eta_z C^{\sigma_z} V_C^{\xi_z} \tag{62}$$

Table 3. Coefficients for the capacitor cost model equation.

Coefficients	Value	Ranges	σ_z	ξ_z
η_0	-0.5651	$(-4.043, 2.913)$	0	0
η_1	7.98×10^{-4}	$(-0.017, 0.019)$	1	0
η_2	0.03	$(-0.022, 0.082)$	0	1
η_3	5.35×10^{-7}	$(-1.6 \times 10^{-5}, 1.74 \times 10^{-53})$	2	0
η_4	3.2×10^{-5}	$(-5 \times 10^{-5}, 0.0001139)$	1	1
η_5	-1.72×10^{-4}	$(-4 \times 10^{-4}, 5.9 \times 10^{-5})$	0	2
η_6	-4.81×10^{-8}	$(-1.1 \times 10^{-7}, 1 \times 10^{-8})$	2	1
η_7	1.6×10^{-7}	$(4.2 \times 10^{-8}, 2.8 \times 10^{-7})$	1	2
η_8	2.5×10^{-7}	$(-5.5 \times 10^{-8}, 5.6 \times 10^{-8})$	0	3

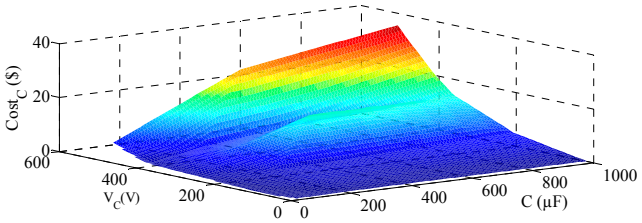

Figure 20. Capacitor cost model for one unit.

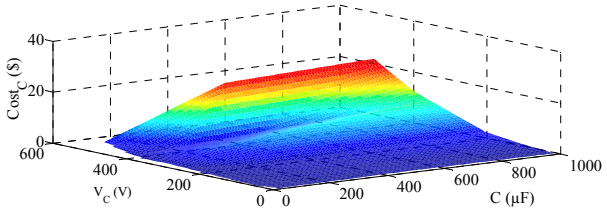

Figure 21. Capacitor cost model for 1000 units.

4.5. Flyback Coupled-Inductor Core

Typical core materials include silicon steel, iron powder and ferrites. A ferrite material core is used in the selected transformer to demonstrate the methodology. Two types of cores, gapped and ungapped, are considered in the proposed cost model with a frequency range between 50 KHz and 500 KHz. High frequency cores which are used for radio or telecommunications application are excluded. The cost core cost model was prepared using f_{sw}, A_L and cost. Figures 22 and 23 show the interpolated $Cost_{CO}$ surfaces while the mathematical model is shown in Equation (63) and its coefficients are shown in Table 4.

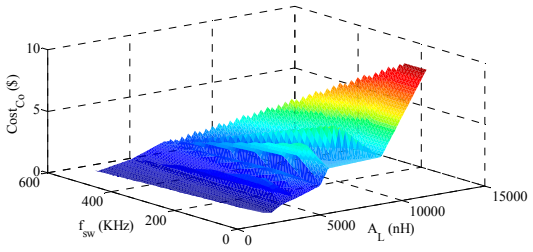

Figure 22. Flyback core cost model for one unit.

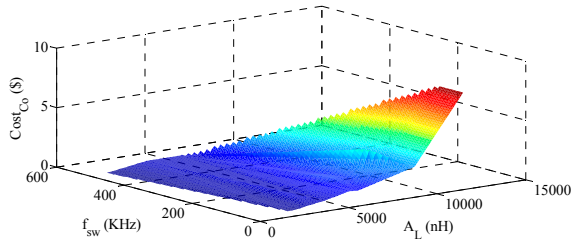

Figure 23. Flyback core cost model for 1000 units.

$$Cost_{Co}(A_L, f_{sw}) = \sum_{m=0}^{m=4} \tau_m A_L^{\psi_m} f_{sw}^{\rho_m} \tag{63}$$

Table 4. Coefficients for the core cost model equation.

Coefficients	Value	Ranges	ψ_m	ρ_m
τ_0	1.204	(0.6736, 1.735)	0	0
τ_1	1.625	(1.31, 1.939)	1	0
τ_2	0.1432	(−0.6245, 0.9078)	0	1
τ_3	−0.007604	(−0.467, 0.4518)	1	1
τ_4	−0.1744	(−0.6827, 0.344)	0	2

Cost models presented here were evaluated based on two criteria. The first criterion is that an analytical form is available for the cost model, i.e., polynomial, trigonometric, exponential, etc. in order to integrate this model with other mathematical and optimization tools. The second criterion is that the R^2 value for each model, which is a measure between 0 and 1 of how well does the model match discrete data points, is acceptable. An R^2 value that is closer to 1 is desired. The second criterion is essential when dealing with cost modeling of power electronic devices since their ratings are not available as continuous options; for example, MOSFET ratings of 50 V and 100 V exist, but not necessarily at 63.5 V, and the surface fit provided applies to the continuous range. All R^2 values of the proposed models are shown in Table 5, and are all acceptable except for MOSFETs whose cost model's R^2 value is low. To mitigate this case, a locally weighted scatterplot smoothing (LOWESS) model was established to achieve an R^2 = 0.9436 for $Cost_M$ but does not have an explicitly model equation like the polynomial one. Also, note that that exact cost estimates of specific components can be obtained if coefficients are changed within the specified ranges shown in Tables 1–4.

Table 5. Surface fitting evaluation of cost models.

Cost Model	R^2 Value (0 to 1)
$Cost_M$ (Polynomial, presented here)	0.6717
$Cost_M$ (LOWESS, no analytical expression)	0.9436
$Cost_D$	0.8899
$Cost_C$	0.8274
$Cost_L$	0.7014
$Cost_{CO}$	0.9365

5. Results

Basic boost, buck and flyback converters were experimentally developed to test the power loss and cost models presented here. Bus bar losses are not considered since the experimental prototype is at a power level that does not require bus bar. More bus bar losses information can be found in [40]. All parasitic elements and specific test condition examples are given in Table 6. Figure 24 shows the board housing both the boost and buck converters (flyback converter not shown).

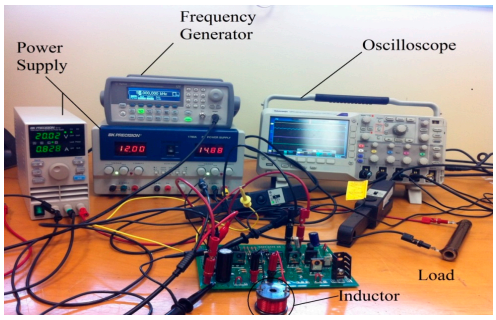

Figure 24. Experimental setup for the buck and boost converters.

Table 6. Example testing conditions and parasitic elements in experimental prototypes.

Parameter	Boost	Buck	Flyback
V_{in}	19.3 V	60 V	12.1 V
I_{in}	3.18 A	1.04 A	0.434 A
V_{out}	75.2 V	24.1 V	25.7 V
I_{out}	0.794 A	2.39 A	0.151 A
Δi	1.1 A	2.95 A	0.89 A
f_{sw}	50 KHz	50 KHz	100 KHz
D	0.75	0.4	0.7
ESR	0.603 Ω	0.603 Ω	0.603 Ω
V_{D0}	1 V	1 V	1 V
R_D	7 mΩ	7 mΩ	7 mΩ
DCR/R_{pri}	0.06 Ω	34 mΩ	0.09
ACR/R_{sec}	0	1.5 Ω	0.58
Q_{rr}	195 nC	195 nC	195 nC
Q_{gs}	64 nC	13 nC	13 nC
R_{DSon}	0.029 Ω	0.18 Ω	0.18 Ω
t_r	100 nsec	51 nsec	51 nsec
t_f	63 nsec	36 nsec	36 nsec
$\approx R_c$	3325 Ω	-	-
L_m, L_{pri}	-	-	59.4 µH, 3.5 µH
B	-	3400 mT	42.42 mT
V_e/A_C	-	0.24 cm^3	0.97 cm^3

Parasitic elements shown in Table 6 are extracted from datasheets of the components used in the experimental setup and which are IRFP4332PBF MOSFET, AIRD-03-101K inductor, MURF860G diode, and EEU-EB2D221 capacitor in the boost converter and IRFP240 MOSFET, AIRD-03-101K inductor, MURF860G diode, and EEU-EB2D221 capacitor in buck converters, and IRFP240 MOSFET, Q4338-BL flyback transformer, EGP10G Diode, and EEU-EB2D221 capacitor are used in the flyback converter.

5.1. Power Loss Model Verification

To validate the power loss models derived in Section 3, each of the three converters was tested under the conditions shown in Table 6, along with various output voltages and currents varied with the duty ratio. Power losses were measured by deducting the output power of the converter from its input power. Gate drive losses can be measured, but were not considered since the gate drive power supply was separate in the experimental setup and the gate drive losses do not contribute to the experimental system-level verification. Voltage divider and current sensor in the prototype consume much less power than main power losses, thus they are not taken into consideration. Figures 25–27 show experimental results of each converter at the specified test conditions in Table 6. Input and output voltage and current were measured to obtain totally converter loss to verify converter scope-level power loss. All measurements are under zero offset condition and using calibrated probes to ensure measurement accuracy.

Tables 7–9 show power loss estimates of each converter under different duty ratios. It is clear from Tables 5–7 that the error in estimating power losses using the derived models is less than 8%

leading to more than 92% accuracy. More accurate measurements and models would still be of very high value for rapid prototyping, but the achieved model-based estimation error is very satisfactory for evaluating various design options. Among the sources of estimation error are approximations, e.g., R_C (when not in a datasheet), and limited measurement accuracy.

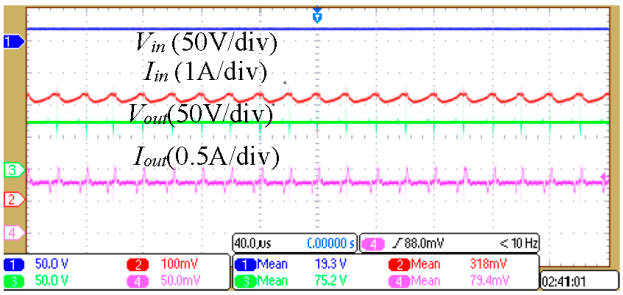

Figure 25. Boost converter experimental results for D = 75%.

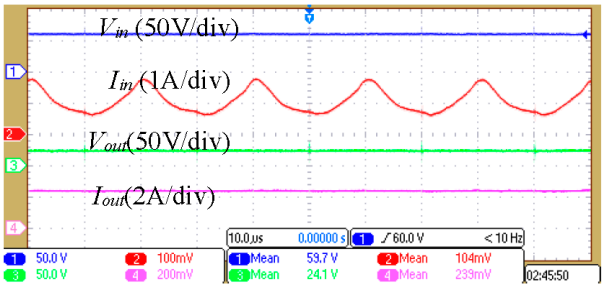

Figure 26. Buck converter experimental results for D = 40%.

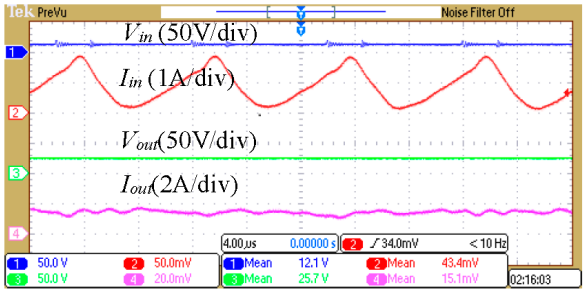

Figure 27. Flyback converter experimental results for D = 50%.

Table 7. Estimated and measured power loss in boost converter.

Duty Ratio	$P_{Measured}$ (W)	$P_{Estimated}$ (W)	Error %
30%	0.6	0.56	−6.6%
40%	0.78	0.72	−7.69%
50%	0.97	0.92	−5.15%
60%	1.36	1.37	0.74%

Table 8. Estimated and measured power loss in buck converter.

Duty Ratio	$P_{Measured}$ (W)	$P_{Estimated}$ (W)	Error %
20%	2.54	2.49	−1.96%
30%	3.76	3.78	0.53%
40%	4.8	5.04	5%
50%	7.05	6.55	−7.09%

Table 9. Estimated and measured power loss in flyback converter.

Duty Ratio	$P_{Measured}$ (W)	$P_{Estimated}$ (W)	Error %
20%	0.32	0.31	−3.13%
30%	0.55	0.56	1.81%
40%	0.85	0.82	−4.7%
50%	1.32	1.27	−3.78%

5.2. Cost Model Verification

In order to validate the cost models proposed in Section 3, prices of the parts used were compared to prices generated from the mathematical models for the MOSFET, diode, inductor, and capacitor utilized. The flyback coupled inductor model was split into wire and cores due to their abundant information, thus similar core and wire to the Q4338-BL model are used for cost validation. Cost figures of these components were generated based on Equations (59)–(63), and results are compared to estimated prices in Table 10.

Table 10. Detailed cost comparison for power components.

Component	Actual Cost	Estimated Cost	Error %
MOSFET (IRFP4332PBF)	$4.33	$4.37	−0.92%
Inductor (AIRD-03-101K)	$5.97	$5.95	0.33%
Diode (MURF860G)	$0.99	$1.03	−4.04%
Capacitor (EEU-EB2D221)	$0.723	$0.752	−4.01%
Core (B66421G0000X187)	$0.69	$0.724	−4.93%
Wire (Belden 22AWG)	$49.03	$48.03	2.039%

Results in Table 10 are shown to have less than 5% error and thus the cost models established prove that the results are more than 95% accurate. The accuracy of the cost model was improved with the help of interpolated graphs and surface fitting tools. Since cost of components changes with technology and manufacturing trends, the methodology presented here can be applied for future technologies or with a refined, more comprehensive database.

6. Optimization of Converter Designs for a Specific Figure of Merit

6.1. Optimal Design Selection Approach

The main objective of establishing power loss models in Sections 3 and 4 is to achieve the capability of selecting the "right components" in a converter. Such components can be selected based on a figure of merit, or an optimization objective function. These figures of merit include two main factors which are (1) minimum power loss; and (2) minimum cost. While co-optimizing for both can establish a Pareto front for acceptable local minima of cost and power loss, the next sections optimize for either power loss or cost, independently. Co-optimization is left for future work and is a natural next step of this paper.

In order to find component combinations that can optimize a figure of merit, a direct search optimization is performed with priority given to the component with most influence on the figure of merit being optimized. In both power loss and cost optimizations, inductors are given priority—(1) In power loss optimization, the impact of inductors on ripple and other components' power losses is very significant; (2) in cost optimization, inductors tend to be the most expensive components. Figure 28 demonstrates the overall high-level direct search optimization performed. Sections 6.2 and 6.3 present approaches for two different figures of merit being power loss and cost, respectively.

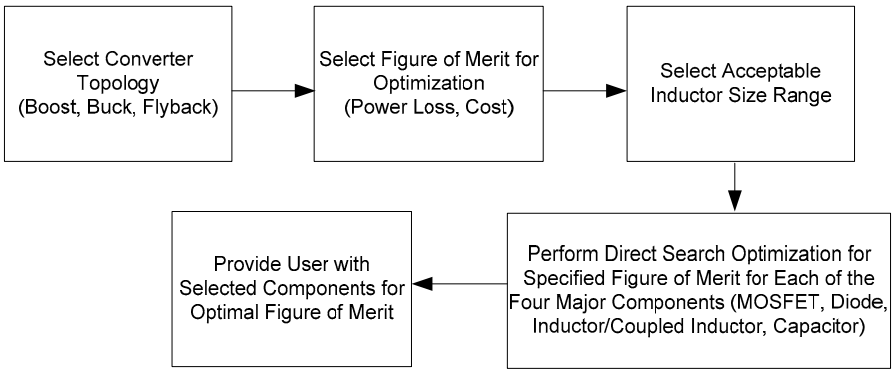

Figure 28. High-level block diagram of proposed figure of merit optimization.

6.2. Minimum Power Loss Designs

Power loss models developed here are combined with converter ratings to automatically produce system-level minimum power loss and select the right components. This procedure reduces the manual effort in calculating component power losses to select a combination of components that minimizes power losses. Components are selected in the order that affects selection of other components—For example, selecting the inductor in a boost converter comes as a priority as it affects the losses in semiconductors and capacitor as the inductor determines the input current ripple. In order to search for components with compatible voltage and current ratings which are set by the designer, minimum inductance and capacitance values in addition to MOSFET and diode ratings for boost and buck converters in CCM are calculated based on [41,42], while component ratings are double the converter ratings even though this factor can be modified. The resulting minimum power loss does not guarantee low cost but selects components leading to a minimum converter power loss from the available database. A pseudo-code is shown below as an example for inductor selection for minimum inductor power loss and similar logic is applied to other components. Figure 29 shows a flowchart for the minimum power loss rapid prototyping tool.

Start
Get input and output parameters;
$I_L = I_{in}$;
$L = ((V_{in} \times D \times (1 - D))/(2 \times f_{sw} \times I_{out}))$;
$L_{max} = 2 \times L$;
Read inductor.xls file and get the entire database;
    for *i = 1 to all database*
        if *L <= inductor values in database &&*
            L_{max} *> inductor values in database*
                if I_L *<= inductor current values in database*
                    Extract ACR, DCR and RC values from the database;
            end if;
        end if;
    i = i + 1;
    end if;
Calculate P_{ACR}, P_{DCR} *and* P_{CORE} *as described in power loss model*
$P_{loss\_inductor} = P_{ACR} + P_{DCR} + P_{CORE}$;
Print component name;

The procedure shown in Figure 29 is integrated into a user-friendly GUI developed in MATLAB for rapid-prototyping. The user enters the converter type, currently boost or buck converter, and sets

the operating points and basic specifications of the converter such as desired output voltage ripple and switching frequency, then receives suggested components based on the minimum combined power loss. This GUI is shown in Figures 30 and 31 for buck and boost optimal component selection, respectively.

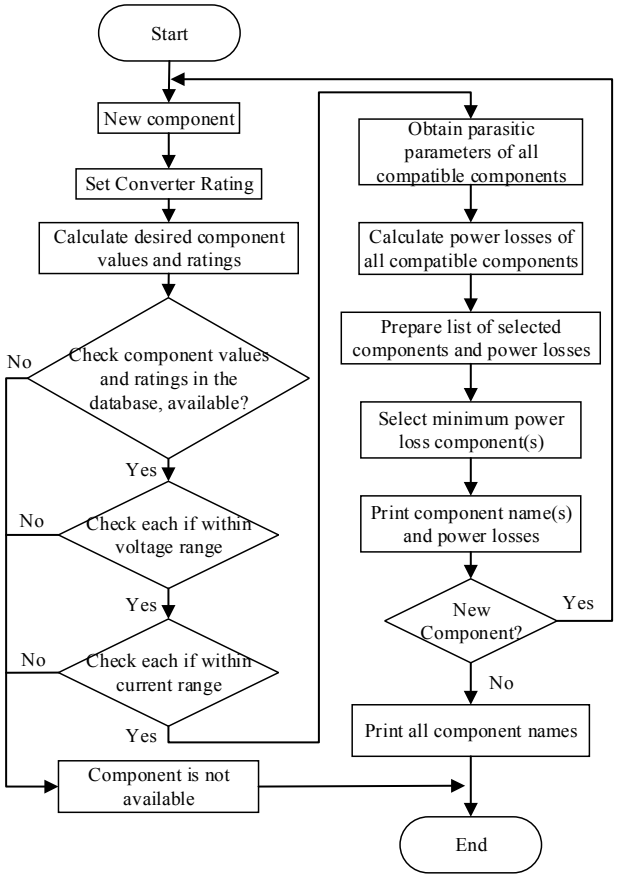

Figure 29. Flowchart of the minimum power loss tool.

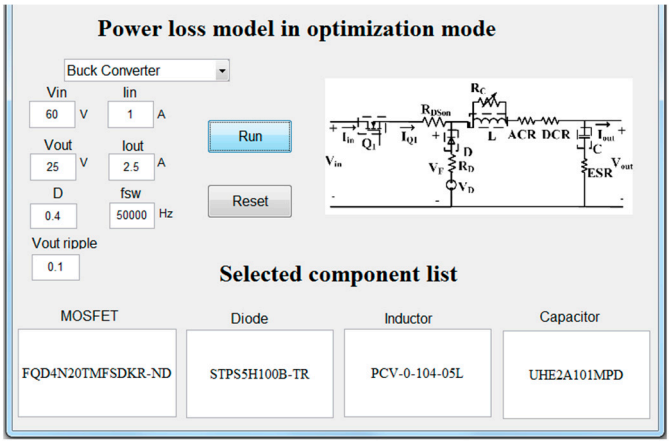

Figure 30. Minimum power loss selection (optimization mode) for a buck converter example.

In order to validate the optimal component selection based on minimum converter power losses, all selected components based on compatible ratings were evaluated manually. Power losses highlighted as gray background in Tables 11 and 12 are those for minimum power loss components and confirm results shown in Figures 30 and 31. Other examples are shown in the Appendix B.

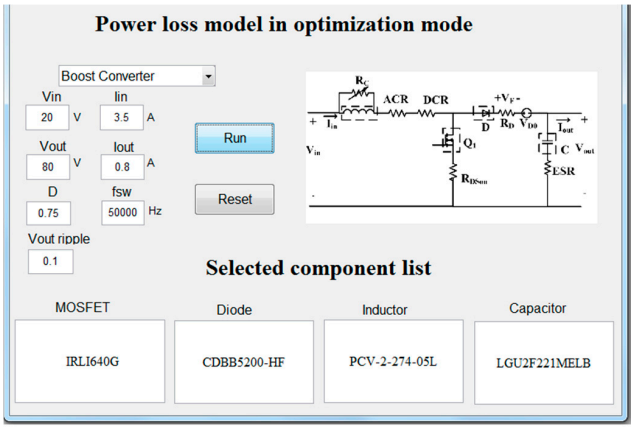

Figure 31. Minimum power loss selection (optimization mode) for a boost converter example.

Table 11. Component options for the buck converter minimum power loss example where shown components have values and/or ratings satisfy converter operating points.

MOSFET		**Diode**	
Suitable Components	P_{Loss} (W)	Suitable Components	P_{Loss} (W)
FQD4N20TMFSCT-ND	5.03508831	SK35A-LTP	2.878
FQD4N20TMFSDKRND	5.03508831	STPS5H100B-TR	2.037
Capacitor		B350A-13-F	2.881
Suitable Components	P_{Loss} (W)	SS35	2.877
UHE2A101MPD	0.005741826	CDBC5100-G	2.464
ESH107M200AM7AA	1.07828776	SB550-E3/54	2.397
UVZ2F101MHD	0.014467593	SK55L-TP	2.464
UPT2G101MHD6	0.014467593	SB550	2.255
Inductor		CDBC580-G	2.458
Suitable Components	P_{Loss} (W)	SS5P10-M3/86A	2.301
PCV-0-104-01L	0.940523683	SB580-T	2.213
PCV-0-104-03L	0.35827212	HSM580G/TR13	2.464
PCV-0-104-05L	0.274278036	RGP30B-E3/73	3.186
		SK310A-LTP	2.890
		CDBA3100-G	2.734
		B3100-13-F	2.586

Table 12. Component options for the boost converter minimum power loss example where shown components have values and/or ratings satisfy converter operating points.

MOSFET		**Capacitor**	
Suitable Components	P_{Loss} (W)	Suitable Components	P_{Loss} (W)
RDN100N20FU6-ND	3.436527778	EEU-EB2D221	0.000223251
RDN100N20-ND	3.436527778	LGU2F221MELB	0.000223251
IRLI640GPBF	1.898888889	ECO-S2GB221EA	0.0271
IRLI640G	1.898888889	**Inductor**	
FQP9N30	4.466997222	Suitable Components	P_{Loss} (W)
STP12NK30Z 3.763864198	3.76386	PCV-0-274-10L	2.983
Diode		PCV-2-274-03L PCV-2-274-05L PCV-2-274-10L PCV-2-394-05L	3.3021
Suitable Components	P_{Loss} (W)	PCV-2-274-05L	1.172
CDBB5200-HF	1.495	PCV-2-274-10L	1.528
		PCV-2-394-05L	3.299

Note that a separate GUI has also been developed for component-specific evaluation as shown in Figure 32, where the effect of specific parameters and component choices can be visualized in terms of power loss.

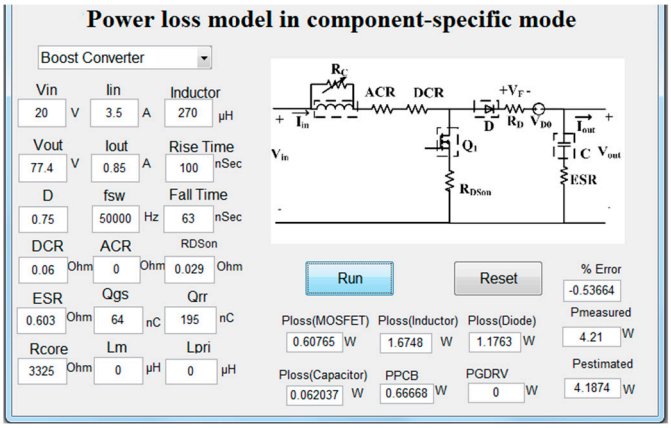

Figure 32. Component-specific power loss model for a boost converter example.

6.3. Minimum Cost Designs

Another rapid prototyping tool is developed to achieve minimum cost of essential components for boost and buck converters as example applications. Component selection for minimum cost is done sequentially for different components based on converter ratings only. A short list of components that satisfy the converter ratings and values for inductance and capacitance is established, and components with minimum cost are selected. This selection is not necessarily optimal in terms of efficiency but ensures minimum cost based on the available database. The optimal-cost component selection pseudo-code is below and the flowchart is shown in Figure 33.

Start
Get input and output parameters;
L = ((V_{in} *×* *D* *×* *(1-D))/(2* *×* f_{sw} *×* I_{out}*));* L_{max} *= 2* *×* *L;*
Read inductor.xls file and get all the database;
  for *i = 1 to all database*
    if *L <= inductor values in database && Lmax > inductor values in database*
      Extract ACR, DCR and RC values from database;
      Extract unit costs and multiple unit costs data base;
    end *i = i + 1;*
  end
Find minimum cost of the component
Print minimum cost of the component for unit quantity;
Calculate P_{ACR}*,* P_{DCR} *and* P_{CORE} *as described in power loss model;*
$P_{loss\_inductor} = P_{ACR} + P_{DCR} + P_{CORE}$*;*
Print component name; Print component cost;

Two GUIs were developed to implement rapid prototyping based on cost models with one GUI targetting minimum converter cost and the other targeting component-specific cost models. Screenshots of the tool designed for rapid prototyping to achieve minimum converter cost are shown in Figures 34 and 35 for buck and boost converters, respectively. Tables 13 and 14 show manual validation of these results based on the short list of components that meet the converter specifications

in the available database. Results in Figures 34 and 35 are highlighted in Tables 13 and 14 for minimum cost. The component-specific GUI is shown in Figure 36.

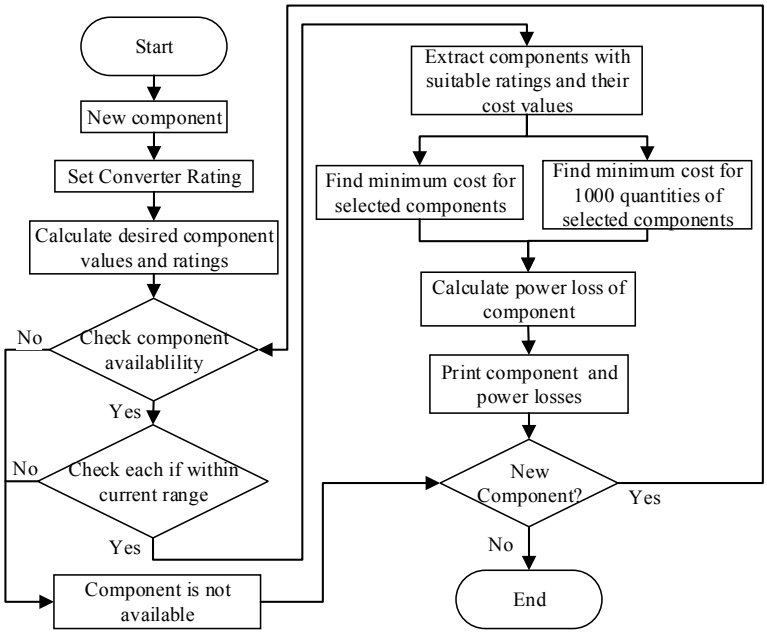

Figure 33. Optimization technique implementation for cost model.

As can be seen in the GUI screenshots and manual validations, the rapid prototyping tools holding all power loss models and cost models from Section 2 are very valuable for practicing engineers and researchers. These GUIs can be conveniently adjusted to include different component types, various technologies for specific components, and a growing database of component with adjustable cost and prices. While models running behind the GUIs may not be all inclusive of all losses in buck and boost converters, the presented methodology and MATLAB platform is very scalable and flexible. Engineers, designers, and researchers can iteratively and manually study the effect of different component parameters, e.g., MOSFET $R_{DS,on}$, on converter efficiency using the component-specific mode, or can rely on built in minimum cost or loss searches in the optimization mode.

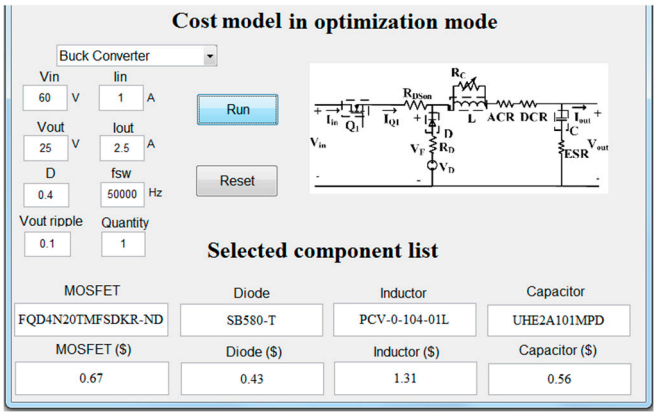

Figure 34. Minimum cost selection (opt. mode) for a buck converter.

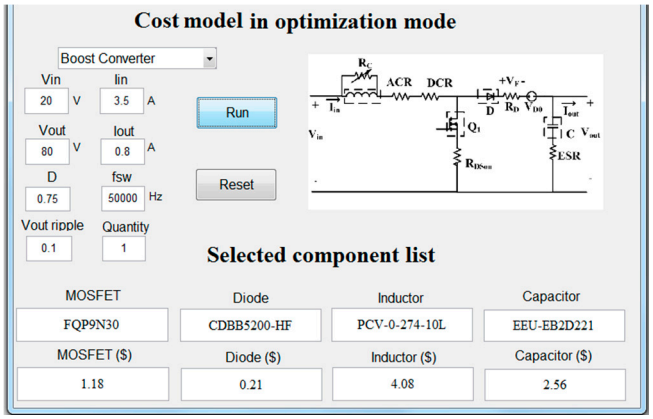

Figure 35. Minimum cost selection (opt. mode) for a buck converter.

Table 13. Component options for the buck converter optimal cost example where shown components have values and/or ratings satisfy converter operating points.

MOSFET		**Diode**	
Suitable Components	*Cost* ($)	Suitable Components	*Cost* ($)
FQD4N20TMFSCT-ND	0.67	SK35A-LTP	0.57
FQD4N20TMFSDKR-ND	0.67	STPS5H100B-TR	1.4
Capacitor		B350A-13-F	0.46
Suitable Components	*Cost* ($)	SS35	0.63
UHE2A101MPD	0.56	B550C-13-F	0.95
ESH107M200AM7AA	1.02	SB550-E3/54	0.61
UVZ2F101MHD	1.85	SK55L-TP	0.49
UPT2G101MHD6	2.68	SB550	0.56
Inductor		CDBC580-G	0.74
Suitable Components	*Cost* ($)	SB580	0.59
PCV-0-104-01L	1.31	SB580-T	0.43
PCV-0-104-03L	1.48	HSM580G/TR13	1.34
PCV-0-104-05L	2.37	RGP30B-E3/73	0.476
		SK310A-LTP	0.57
		CDBA3100-G	0.63
		B3100-13-F	0.68
		CDBC5100-G	0.74
		SS5P10-M3/86A	0.77
		SB5100-T	0.74

Table 14. Component options for the boost converter optimal cost example where shown components have values and/or ratings satisfy converter operating points.

MOSFET		
Suitable Components	*Cost* ($)	P_{Loss} (W)
RDN100N20FU6-ND	2.73	3.436
RDN100N20-ND	2.73	3.436
IRLI640GPBF	2.88	1.898
IRLI640G	2.88	1.898
FQP9N30	1.18	4.467
STP12NK30Z	1.95	3.763864198
Diode		
Suitable Components	*Cost* ($)	P_{Loss} (W)
CDBB5200-HF	0.21	1.495

Table 14. *Cont.*

Inductor		
Suitable Components	*Cost* ($)	P_{Loss} (W)
PCV-0-274-10L		
PCV-2-274-03L		
PCV-2-274-05L		
PCV-2-274-10L		
PCV-2-394-05L		
PCV-2-274-03L	4.15	3.302
PCV-2-274-05L	4.56	1.172
PCV-2-274-10L	7.39	1.528
PCV-2-394-05L	5.1	3.299
Capacitor		
Suitable Components	*Cost* ($)	P_{Loss} (W)
EEU-EB2D221	2.56	0.000223251
LGU2F221MELB	7.022	0.000223251
ECO-S2GB221EA	4.68	0.0271

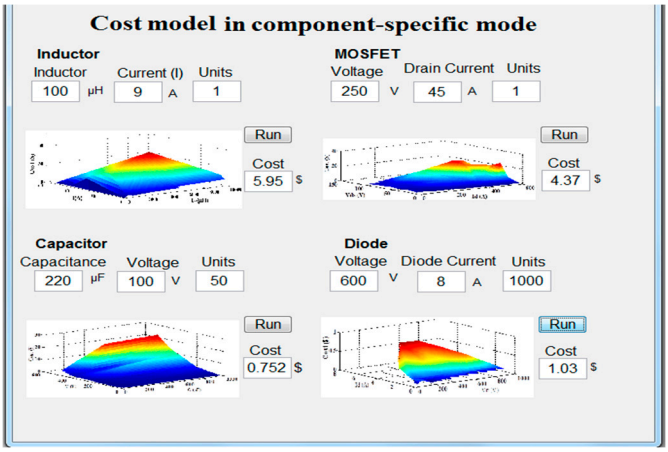

Figure 36. GUI for component cost estimates in component-specific mode.

7. Conclusions

This paper presents power loss and cost models of major power electronic components which can be further aggregated into power electronic converters. The proposed models are expected to aid designers in making preliminary useful estimates which help to decide specific components that can achieve desired system power loss and cost. Cost models are found based on an extensive survey of commercial devices followed by cost surface fitting. Power loss models are based on generalized forms that are reformulated to reach converter-specific models. Power loss models presented here are based on non-idealities and parasitic elements including PCB and gate drive losses to develop to achieve higher accuracy. The presented models are shown to be over 93% accurate. All models are integrated into MATLAB-based rapid prototyping tools designed for either minimum power loss or minimum cost component selection. With a large database, hundreds or thousands of various component options can be evaluated in minutes to achieve model-based component selection for optimized converter designs. The implementation of these tools with supplier databases is of major future interest, and extending the models to other applications and converters such as DC/AC inverters and AC/DC rectifiers can be achieved using the methodologies proposed here. Future work will include open-access web-based GUIs and possible linking to major supplier databases for up-to-date component lists that eliminate obsolete parts, and up-to-date prices.

Author Contributions: Amruta V. Kulkarni is the first author of this paper whose Master's thesis work focused on the topic of the paper; she performed the literature review to find all related cost and loss model equations, applied

these equations to specific converter topologies, and built the rapid prototyping tools; she also established the original component database. Weiqiang Chen helped to perform the hardware validation of models and double checked the accuracy of cost and loss models in addition to database data; he was responsible for paper submission and revision. Ali M. Bazzi provided the original idea for this paper, and provided guidance and mentoring on how to achieve the rapid prototyping tools; he was the research and academic advisor of Amruta V. Kulkarni and the advisor of Weiqiang Chen.

Conflicts of Interest: The authors declare no conflict of interest.

Abbreviations

The following abbreviations are used in this manuscript:

A	Plate area in mm^2
A_C	Core cross-sectional area
A_L	Inductance factor
ACR	Inductor ac resistance
B	The peak flux density
$B^{\beta}{}_{AC}$	AC component of flux density
ΔB^m, ΔB_{max}	Maximum peak flux density
C	Capacitance value
C_{gs}	MOSFET gate-to-source capacitance
$Cost_C$	Capacitor cost model
$Cost_{CO}$	Core cost model
$Cost_D$	Diode cost model
$Cost_L$	Inductor cost model
$Cost_M$	MOSFET cost model
$Cost_W$	Wire cost model
C_{sn}	Snubber capacitor
C_{stray}	PCB stray capacitance
d	Plate separation in mm
D	Duty ratio
DCR	Inductor DC resistance
D_{sn}	Snubber diode
E_r	Dielectric constant for air
ESR	Equivalent series resistance
f	Inductor Current frequency
f_{sw}	Switching frequency
G	Wire gauge
H	Height of PCB trace
Δi	Inductor ripple current
I_{Crms}	Capacitor RMS current
I_{Drms}, I_D	Drain-to-source RMS current
I_{Don}, I_{Doff}	MOSFET on- and off-current
ΔI_F	Change in diode forward current
I_{Favg}, I_{Frms}	Diode avg. and RMS fwd. current
$I_{Dsn(avg)}$	Snubber diode average current
$I_{Dsn(rms)}$	Snubber diode RMS current
I_{in}	Converter input current
I_L	Inductor current
I_{Lavg}, I_{Lrms}	Inductor avgerage and RMS current
I_{out}	Converter output current
I_{QBS}, I_{QCC}	Gate drive quiescent currents
I_{Srms}	Snubber branch RMS current
I_{trace}	PCB trace current
K_1	Inductor core material constant
K_{fe}	Inductor current material constant at f_{sw}
L	Inductance value in
L_e	Length of PCB trace
L_m	Mutual inductance
L_{pri}	Primary inductance
L_{sec}	Secondary inductance
L_{stray}	PCB stray inductance
n	Transformation ratio
N_{pri}	Primary windings number of turns
N_{sec}	Secondary windings number of turns

P_{ac}	Capacitor AC loss
P_{ACR}	Inductor AC resistance loss
P_{BT}	Power dissipated at the bootstrap pin
P_{CD}	Diode conduction loss
P_{CDsn}	Snubber diode power loss
P_{clamp}	Power loss in the clamp unit
P_{CM}	MOSFET conduction loss
P_{CORE}	Inductor or flyback transformer core loss
P_{Cstray}	PCB stray capacitance loss
P_{dc}	Capacitor DC loss
P_{DCR}	Inductor DC resistance loss
P_G	MOSFET gate loss
P_{GDRV}	Gate drive power loss
$P_{loss(Capacitor)}$	Total capacitor power loss
$P_{loss(Diode)}$	Total diode power loss
$P_{loss(Inductor)}$	Total inductor power loss
$P_{loss(MOSFET)}$	Total MOSFET power loss
$P_{ON(M)}$	MOSFET turn-on loss
$P_{OFF(M)}$	MOSFET turn-off loss
P_{PCB}	Total PCB power loss
P_{Rpri}	Flyback transformer primary power loss
P_{Rsec}	Flyback transformer secondary power loss
P_{stray}	PCB stray inductance power loss
P_{SW}	MOSFET total switching losses
P_{SWD}	Diode switching loss
P_{SWDsn}	Snubber diode switching loss
P_{Total}	Total converter power loss
P_{trace}	PCB trace power loss
P_{VCC}	Power drawn through the gate drive supply pin
Q_g	Bootstrap capacitor charge
Q_{gs}	Gate-to-source charge
Q_{rr}	Diode reverse recovery charge
R_C	Effective core impedance
R_{Dsn}	Snubber diode on-resistance
R_D	Diode on-resistance
R_{DSon}	Drain-to-source resistance
R_{Load}	Output load resistor
R_{sn}	Snubber resistor
R_p	Capacitor parallel resistor
R_{pri}	Primary DC resistance
R_{sec}	Secondary DC resistance
R_{trace}	PCB trace resistance
t_r, t_f	MOSFET rise and fall times
V_B	Diode DC blocking voltage
V_{BT}	Gate drive IC Bootstrap voltage
V_C	Capacitor voltage
V_{clamp}	Clamp voltage rise
V_{CC}	Gate drive IC Supply voltage
V_d	Voltage difference between dielectric material
V_{D0}, V_{Dsn0}	Diode initial state voltage
V_{Dmax}, V_{Dtyp}	Diode maximum and typical fwd. voltage
V_{DS}, V_{ds}	Drain to source voltage
V_{DSBR}	Drain to source breakdown voltage
V_e	Effective core volume
ΔV_F	Change in diode fwd. voltage
V_{in}	Converter input voltage
V_L	Inductor voltage
V_{out}	Converter output voltage
ΔV_{out}	Converter output voltage ripple
V_{rr}	Reverse recovery voltage
V_{supply}	Supply voltage
W	Width of PCB trace
x, y	Core loss coefficients

Appendix A

Examples of optimal component selection are shown here with highlighted values matching results of the rapid prototyping tools. Table A1 shows the example cases of boost and buck converter specifications, the parameters shown in Table A1 are the bases of the calculation of power loss and cost. Afterwards, the minimum power loss and cost can be found and optimal components can be selected. Tables A2–A7 show the optimal component selection for power loss minimization and Tables A8–A13 show the optimal component selection for cost minimization.

Table A1. Example cases of boost and buck converter specifications.

Parameters	Boost Converter			Buck Converter		
	Case 1	**Case 2**	**Case 3**	**Case 1**	**Case 2**	**Case 3**
V_{in} (V)	50	40	20	50	200	200
I_{in} (A)	4	2.1	2	0.5	2	1.5
V_{out} (V)	120	80	130	25	160	120
I_{out} (A)	2.1	0.9	0.3	1	2.5	2.5
$Duty$	0.6	0.5	0.85	0.5	0.8	0.6
f_{sw} (KHz)	100	100	50	50	50	100
$V_{outripple}$ (V)	0.1	0.1	0.1	0.2	0.1	0.2

Table A2. Boost converter minimum loss results for case 1.

MOSFET		**Diode**	
Suitable Components	P_{Loss} (W)	Suitable Components	P_{Loss} (W)
FQP9N30	6.05	RD0504T-TL-H	3.63
STP12NK30Z	4.19	BY229B-400HE3/45	5.53
IRF740PBF	5.87	STTH5L04DEE-TR	3.26
IRF740STRLPBF	5.87	**Capacitor**	
SiHB10N40D	6.14	Suitable Components	P_{Loss} (W)
Inductor		LGU2F221MELB	0.00022
Suitable Components	P_{Loss} (W)	ECO-S2GB221EA	0.027
PCV-2-274-03L	4.42		
PCV-2-274-05L	1.60		
PCV-2-274-10L	2.05		

Table A3. Boost converter minimum loss results for case 2.

MOSFET		**Inductor**	
Suitable Components	P_{Loss} (W)	Suitable Components	P_{Loss} (W)
FQD7N20LTMDKR	2.47	PCV-2-394-05L	1.32
BUZ73AL H-ND	1.86		
JAN2N6798U-MIL	1.28		
FQD7N30TMTR-ND	2.027	**Capacitor**	
Diode		Suitable Components	P_{Loss} (W)
Suitable Components	P_{Loss} (W)	EEU-ED2C470	0.00022
S320	1.77	UPB2E470MHD1TO	0.00022
PDS3200-13	1.66	ECO-S2GA470BA	0.022
GI912-E3/73	2.01	380LX470M500H012	0.0055

Table A4. Boost converter minimum loss results for case 3.

MOSFET		**Diode**	
Suitable Components	P_{Loss} (W)	Suitable Components	P_{Loss} (W)
FQD7N30TMTR-ND	2.51	UVZ2F101MHD	0.00019
IRF730PBF	3.46	UPT2G101MHD6	0.00019
IRF730STRRPBF	3.46	**Inductor**	
STP7NK40Z	3.45	Suitable Components	P_{Loss} (W)
STD9NM40N	2.72	PCV-2-564-02L	12.71
STD6NK50ZT4	4.16	PCV-2-564-06L	8.05
FDD6N50FTM	4.00	PCV-2-564-08L	4.25
NDF05N50ZH	5.17	DO5040H-684KLB	37.93
Diode			
Suitable Components	P_{Loss} (W)		
RGP30G-E3/73	0.64		

Table A5. Buck converter minimum loss results for case 1.

MOSFET		**Inductor**	
Suitable Components	P_{Loss} (W)	Suitable Components	P_{Loss} (W)
FQT7N10LTFCT-ND	0.43	PCV-2-223-05L	0.05
FQT7N10LTFDKR-ND	0.43	PCV-2-223-10L	0.049
FQT7N10TFTR-ND	0.30	RFB1010-221L	3.48
ZXMN20B28KTCCTN	0.66	CV-0-224-03L	0.14
ZXMN20B28KTCDKR	0.66		
Diode			
Suitable Components	P_{Loss} (W)		
SS15	0.95	**Capacitor**	
GF1A-E3/67A	1.096	Suitable Components	P_{Loss} (W)
SS15E-TP	0.89	EEU-FC2A220	0.074
SK15-13-F	0.91	EKXG401ELL220	0.25
SS18-TP	0.84	EEU-EB2D220	0.16
SS18	0.95	UPJ2F220MHD1TN	0.21
B180-13-F	0.92		
CDBA180-G	0.96		
RS1B-E3/5AT	1.17		
CDBM1100-G	0.96		
SS110-TP	0.84		
SB1100	0.96		

Table A6. Buck converter minimum loss results for case 2.

MOSFET		**Diode**	
Suitable Components	P_{Loss} (W)	Suitable Components	P_{Loss} (W)
IRF730PBF	7.084	RGP30G-E3/73	1.16
IRF730STRRPBF	7.084	RD0504T-TL-H	1.037
STP7NK40Z	7.038	STTH5L04DEE-TR	0.87
STD9NM40N	5.47	BYC5DX-500,127	1.062
STD6NK50ZT4	8.63	RGP30J-E3/73	1.075
FDD6N50FTM	8.41	CN649	0.98
NDF05N50ZH	10.47	LXA03B600	1.75
STP8N80K5	6.94	BYV25D-600,118	0.98
SPD06N80C3	6.73	LQA05TC600	1.28
IXTH6N80A	10.77	**Capacitor**	
Inductor		Suitable Components	P_{Loss} (W)
Suitable Components	P_{Loss} (W)	UPT2G101MHD6	0.013
PCV-2-223-05L	0.19		
PCV-2-223-10L	0.17		
PCH-27X-223_LT	136.30		
PCV-0-224-03L	1.048		

Table A7. Buck converter minimum loss results for case 3.

MOSFET		**Diode**	
Suitable Components	P_{Loss} (W)	Suitable Components	P_{Loss} (W)
IRF720	9.74	RGP30G-E3/73	2.27
IRF720SPBF	9.74	RD0504T-TL-H	2.018
IRF720STRRPBF	9.74	STTH5L04DEE-TR	1.74
IRF730PBF	5.83	**Inductor**	
IRF730STRRPBF	5.83	Suitable Components	P_{Loss} (W)
STP7NK40Z	5.74	PCV-0-104-01L	4.63
STD9NM40N	4.36	PCV-0-104-03L	1.75
STD6NK50ZT4	7.26	PCV-0-104-05L	1.34
FDD6N50FTM	7.24	**Capacitor**	
NDF05N50ZH	8.43	Suitable Components	P_{Loss} (W)
STP8N80K5	5.95	UPB2E470MHD1TO	0.021
SPD06N80C3	5.96	ECO-S2GA470BA	2.058
IXTH6N80A	9.883333333	380LX470M500H012 380LX470M500H012	0.520833

Table A8. Boost converter minimum cost results for case 1.

MOSFET		**Diode**	
Suitable Components	*Cost* ($)	Suitable Components	*Cost* ($)
FQP9N30	1.18	RD0504T-TL-H	1.05
STP12NK30Z	1.95	BY229B-400HE3/45	1.03
IRF740PBF	1.63	BYC5DX-500,127	0.35
IRF740STRLPBF	1.63	BYV25D-600,118	0.848
SiHB10N40D	1.79	LQA05TC600	1.41
Inductor		MURF860G	0.99
Suitable Components	*Cost* ($)	LQA08TC600	1.93
PCV-2-274-03L	4.15	QH08TZ600	1.85
PCV-2-274-05L	4.56	**Capacitor**	
P CV-2-274-10L	7.39	Suitable Components	*Cost* ($)
		LGU2F221MELB	7.022
		ECO-S2GB221EA	4.68

Table A9. Boost converter minimum cost results for case 2.

MOSFET		**Diode**	
Suitable Components	*Cost* ($)	Suitable Components	*Cost* ($)
FQD7N20LTMDKR-ND	0.98	GI912-E3/73	0.48
BUZ73AL H-ND	1.26	RGP30G-E3/73	0.45
JAN2N6798U-MIL	4.34	RD0504T-TL-H	1.05
RDN100N20FU6-ND	2.73	**Capacitor**	
RDN100N20-ND	2.73	Suitable Components	*Cost* ($)
IRLI640GPBF	2.88	EEU-ED2C470	0.72
IRLI640G	2.88	UPB2E470MHD1TO	1.67
FQD7N30TMTR-ND	1.04	ECO-S2GA470BA	1.31
FQP9N30	1.18	380LX470M500H012	5.41
STP12NK30Z	1.95	**Inductor**	
		Suitable Components	*Cost* ($)
		PCV-2-394-05L	5.1

Table A10. Boost converter minimum cost results for case 3.

MOSFET		**Inductor**	
Suitable Components	*Cost* ($)	Suitable Components	*Cost* ($)
FQD7N30TMTR-ND	1.04	PCV-2-564-02L	3.78
FQP9N30	1.18	PCV-2-564-06L	6.46
STP12NK30Z	1.95	PCV-2-564-08L	10.79
IRF730PBF	1.26	**Capacitor**	
IRF730STRRPBF	1.51	Suitable Components	*Cost* ($)
STP7NK40Z	1.56	UVZ2F101MHD	1.85
STD9NM40N	1.67	UPT2G101MHD6	2.68
IRF740PBF	1.63		
IRF740STRLPBF	1.63	**Diode**	
SiHB10N40D	1.79	Suitable Components	*Cost* ($)
STD6NK50ZT4	1.18	LQA05TC600	1.41
FDD6N50FTM	1.1	RGP30G-E3/73	0.45
NDF05N50ZH	0.94	RD0504T-TL-H	1.05
TK10A50D	1.89	BYC5DX-500,127	0.35
STP11NK50ZFP	1.93	RGP30J-E3/73	0.495
IPA50R350CP	1.12	LXA03B600	0.81
FDPF12N50UT	1.73	BYV25D-600,118	0.848

Table A11. Buck converter minimum cost results for case 1.

MOSFET		**Inductor**	
Suitable Components	*Cost* ($)	Suitable Components	*Cost* ($)
FQT7N10LTFCT-ND	0.54	PCV-2-223-05L	2.12
FQT7N10LTFDKR-ND	0.54	PCV-2-223-10L	2.06
FQT7N10TFTR-ND	0.54	PCH-27X-223_LT	1.91
Diode		RFB1010-221L	0.68
Suitable Components	*Cost* ($)	PCV-0-224-03L	1.46
SS18-TP	0.39	**Capacitor**	
SS18	0.46	Suitable Components	*Cost* ($)
B180-13-F	0.82	EEU-FC2A220	0.502
CDBA180-G	0.54	EKXG401ELL220	1.72
RS1B-E3/5AT	0.178	EEU-EB2D220	0.69
CDBM1100-G	0.57	UPJ2F220MHD1TN	1.324
SS110-TP	0.39		
SB1100	0.52		

Table A12. Buck converter minimum cost results for case 2.

MOSFET		**Diode**	
Suitable Components	*Cost* ($)	Suitable Components	*Cost* ($)
IRF730PBF	1.26	RGP30G-E3/73	0.45
IRF730STRRPBF	1.51	RD0504T-TL-H	1.05
STP7NK40Z	1.56	STTH5L04DEE-TR	1.49
STD9NM40N	1.67	BYC5DX-500,127	0.35
STD6NK50ZT4	1.18	RGP30J-E3/73	0.49
FDD6N50FTM	1.1	CN649	0.45
NDF05N50ZH	0.94	LXA03B600	0.81
Inductor		BYV25D-600,118	0.84
Suitable Components	*Cost* ($)	LQA05TC600	1.41
PCV-2-223-05L	2.12		
PCV-2-223-10L	2.06	**Capacitor**	
PCH-27X-223_LT	1.91	Suitable Components	*Cost* ($)
PCV-0-224-03L	1.46	UPT2G101MHD6	2.68

Table A13. Buck converter minimum cost results for case 3.

MOSFET		**Diode**	
Suitable Components	*Cost* ($)	Suitable Components	*Cost* ($)
IRF720	3.18	RGP30G-E3/73	0.45
IRF720SPBF	1.51	RD0504T-TL-H	1.05
IRF720STRRPBF	1.51	STTH5L04DEE-TR	1.49
IRF730PBF	1.26	**Inductor**	
IRF730STRRPBF	1.51	Suitable Components	*Cost* ($)
STP7NK40Z	1.56	PCV-0-104-01L	1.31
STD9NM40N	1.67	PCV-0-104-03L	1.48
STD6NK50ZT4	1.18	PCV-0-104-05L	2.37
FDD6N50FTM	1.1	**Capacitor**	
NDF05N50ZH	0.94	Suitable Components	*Cost* ($)
		UPB2E470MHD1TO	1.67
		ECO-S2GA470BA	1.31
		380LX470M500H012 380LX470M500H012	5.41

Appendix B

Appendix B.1 PCB Losses

It is important to consider PCB power losses to achieve accuracy in the power loss modeling. Stray inductances and capacitances are usually observed in multilayer PCBs [18–20] and are illustrated in Figure B1.

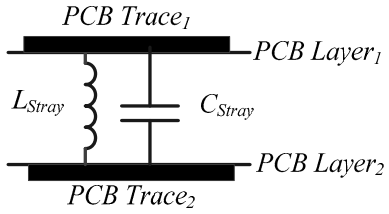

Figure B1. PCB equivalent model.

Trace power loss P_{trace} [17] is calculated as:

$$P_{trace} = I_{trace}^2 R_{trace} \tag{B1}$$

while the stray inductance loss P_{Lstray} is obtained [25] as:

$$P_{Lstray} = I_{trace} L_{stray} \left(\frac{di}{dt} \right) \tag{B2}$$

where L_{stray} can be estimated in μH as:

$$L_{stray} = 2 \times 10^{-4} L_e \left[\ln \left(\frac{2L_e}{W+H} \right) + 0.2 \left(\frac{W+H}{L_e} \right) + 0.5 \right] \tag{B3}$$

As presented in [17], stray capacitance is estimated as:

$$C_{stray} = \frac{0.085 E_r A}{d} \tag{B4}$$

and P_{Cstray} is:

$$P_{Cstray} = \frac{1}{2} V_d^2 C_{Stray} f_{sw} \tag{B5}$$

The total PCB power loss P_{PCB} is thus:

$$P_{PCB} = P_{trace} + P_{Lstray} + P_{Cstray} \tag{B6}$$

Appendix B.2 Gate Drive Losses

Major power loss in the gate drive circuit is normally observed across its supply and bootstrap capacitor pins. Figure B2 shows a typical high-side gate drive IC connection. Gate drive losses shown in this paper mainly focused on self-oscillating ICs or dedicated application ICs.

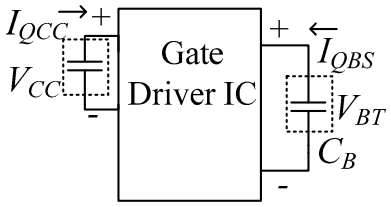

Figure B2. Gate drive ICs equivalent model.

P_{GDRV} is calculated as in [21] to be:

$$P_{GDRV} = P_{VCC} + P_{BT} \tag{B7}$$

where:

$$P_{VCC} = I_{QCC} V_{CC} \tag{B8}$$

$$P_{BT} = I_{QBS} V_{BT} \tag{B9}$$

The converter total power loss P_{Total} is thus:

$$P_{Total} = P_{loss(MOSFET)} + P_{loss(Inductor)} + P_{loss(Diode)} + P_{loss(Capacitor)} + P_{PCB} + P_{GDRV} \tag{B10}$$

References

1. Ma, K.; Blaabjerg, F. Modulation methods for neutral-point-clamped wind power converter achieving loss and thermal redistribution under low-voltage ride-through. *IEEE Trans. Ind. Electron.* **2014**, *61*, 835–845. [CrossRef]
2. Zhang, Z.; Yu, L.; Sun, L.; Qian, L.; Huang, X. Iron loss analysis of doubly salient brushless DC generators. *IEEE Trans. Ind. Electron.* **2015**, *62*, 2156–2163. [CrossRef]
3. Pyrhönen, J.; Ruoho, S.; Nerg, J.; Paju, M.; Tuominen, S.; Kankaanpaa, H.; Stern, R.; Boglietti, A.; Uzhegov, N. Hysteresis losses in sintered NdFeB permanent magnets in rotating electrical machines. *IEEE Trans. Ind. Electron.* **2015**, *62*, 857–865. [CrossRef]
4. Piris-Botalla, L.; Oggier, G.G.; Airabella, A.M.; García, G.O. Power losses evaluation of a bidirectional three-port DC-DC converter for hybrid electric system. *Int. J. Electr. Power Energy Syste.* **2014**, *58*, 1–8. [CrossRef]
5. Jahdi, S.; Alatise, O.; Alexakis, P.; Ran, L.; Mawby, P. The impact of temperature and switching rate on the dynamic characteristics of silicon carbide schottky barrier diodes and MOSFETs. *IEEE Trans. Ind. Electron.* **2015**, *62*, 163–171. [CrossRef]
6. Bazzi, A.M.; Krein, P.T.; Kimball, J.W.; Kepley, K. IGBT and diode loss estimation under hysteresis switching. *IEEE Trans. Power Electr.* **2012**, *27*, 1044–1048. [CrossRef]
7. Lu, X.; Wan, J. Modeling and control of the distributed power converters in a standalone DC microgrid. *Energies* **2016**, *9*, 217. [CrossRef]

8. Locment, F.; Sechilariu, M. Modeling and simulation of DC microgrids for electric vehicle charging stations. *Energies* **2015**, *8*, 4335–4356. [CrossRef]
9. Sekar, A.; Raghavan, D. Implementation of single phase soft switched PFC converter for plug-in-hybrid electric vehicles. *Energies* **2015**, *8*, 13096–13111. [CrossRef]
10. Lai, C.-M. Development of a novel bidirectional DC/DC converter topology with high voltage conversion ratio for electric vehicles and DC-microgrids. *Energies* **2016**, *9*, 410. [CrossRef]
11. Liu, J.; Chen, W.; Zhang, J.; Xu, D.; Lee, F.C. Evaluation of power losses in different CCM mode single-phase boost FC converters via a simulation tool. In Proceedings of the IEEE Industry Applications Conference, Chicago, IL, USA, 30 September–4 October 2001; pp. 2455–2459.
12. Figueiredo, J.P.M.; Tofoli, F.L.; Alves, R.L. Comparison of non-isolated DC-DC converters from the efficiency point of view. In Proceedings of the IEEE Power Electronics Conference, Orlando, FL, USA, 9–13 October 2011; pp. 14–19.
13. Berringer, K.; Marvin, J.; Perruchoud, P. Semiconductor power losses in AC inverters. In Proceedings of the IEEE IAS Industry Applications Society Annual Meeting, Orlando, FL, USA, 8–12 October 1995; pp. 882–888.
14. Lopez, T.; Elferich, R. Method for the analysis of power MOSFET losses in a synchronous buck converter. In Proceedings of the IEEE Power Electronics and Motion Control Conference, Portoroz, Slovenia, 30 August–1 September 2006; pp. 44–49.
15. Ivanovic, Z.; Blanusa, B.; Knezic, M. Power loss model for efficiency improvement of boost converter. In Proceedings of the Information, Communication and Optimization Technologies, Dijon, France, 21–23 June 2011; pp. 1–6.
16. Bartal, P.; Nagy, I. On-line efficiency estimation for DC-DC converter cluster by dedicated software. In Proceedings of the Energy Conference and Exhibition, Florence, Italy, 9–12 September 2012; pp. 800–805.
17. Bai, Y.-W.; Kuo, W.-C. Design and implementation of an automatic measurement system for DC-DC converter efficiency on a motherboard. In Proceedings of the IEEE Industrial Electronics Society Conference, Glendale, AZ, USA, 7–10 November 2010; pp. 1323–1328.
18. Lope, I.; Carretero, C.; Acero, J.; Burdio, J.M.; Alonso, R. Practical issues when calculating AC losses for magnetic devices in PCB implementations. In Proceedings of the IEEE Applied Power Electronics Conference and Exposition, Orlando, FL, USA, 5–9 February 2012; pp. 1017–1022.
19. Erickson, R.W. *Fundamentals of Power Electronics*, 2nd ed.; Kluwer Academic Publishers: Norwell, MA, USA, 2001.
20. Zumbahlenas, H. *Linear Circuit Design Handbook*, 2nd ed.; Elsevier Publication: Amsterdam, The Netherlands, 2008; pp. 821–895.
21. Fomani, A.A.; Ng, J.C.W.; Shorten, A. An integrated segmented gate driver with adjustable driving capability. In Proceedings of the IEEE Energy Conversion Congress and Exposition, Atlanta, GA, USA, 12–16 September 2010; pp. 2430–2433.
22. Monfareda, M.; Rastegarb, H. Design and experimental verification of a dead beat power control strategy for low cost three phase PWM converters. *Int. J. Electr. Power Energy Syst.* **2012**, *42*, 418–425. [CrossRef]
23. Kim, P.-S. Cost modeling of battery electric vehicle and hybrid electric vehicle based on major parts cost. In Proceedings of the IEEE Power Electronics and Drive Systems Conference, Singapore, Singapore, 17–20 November 2003; pp. 1295–1300.
24. Manimekalai, P.; Harikumar, R. Design, cost estimation and simulation of a standalone PV power generation system using interleaved converter. In Proceedings of the IEEE Emerging Trends in Science, Engineering and Technology, Tiruchirappalli, India, 13–14 December 2012; pp. 416–421.
25. Burkart, R.; Kolar, J.W. Component cost models for multi-objective optimizations of switched-mode power converters. In Proceedings of the IEEE Energy Conversion Congress and Exposition Conference, Denver, CO, USA, 15–19 September 2013; pp. 2139–2146.
26. Sagneri, A.D.; Anderson, D.I.; Perreault, D.J. Optimization of integrated transistors for very high frequency DC-DC converters. *IEEE Trans. Power Electr.* **2013**, *28*, 3614–3626. [CrossRef]
27. Bertoni, N.; Frattini, G.; Massolini, R.; Pareschi, F.; Rovatti, R.; Setti, G. An analytical approach for the design of class-E resonant DC-DC converters. *IEEE Trans. Power Electr.* **2016**. [CrossRef]
28. Kulkarni, A.V.; Bazzi, A.M. A building-block approach to efficiency and cost models of power electronic systems. In Proceedings of the IEEE Applied Power Electronics Conference and Exposition, Fort Worth, TX, USA, 16–20 March 2014; pp. 2727–2734.

29. Krein, P.T. *Elements of Power Electronic*, 2nd ed.; Oxford University Press, Inc.: New York, NY, USA, 1997.
30. Rashid, M.H. *Power Electronics Handbook-Devices, Circuits and Applications*, 2nd ed.; Academic Press: Cambridge, MA, USA, 2007.
31. Chen, J. Need to estimate buck converter efficiency in portable apps? *EE Times-India*. 14 January 2008. Available online: http://www.eetimes.com/document.asp?doc_id=1275090 (accessed on 26 June 2016).
32. Johnson, G.L. *Solid State Tesla Coil*. Available online: http://g3ynh.info/zdocs/refs/Tesla/Johnson2001_ssTeslacoil.pdf (accessed on 26 June 2016).
33. Zhang, X.; Ruan, X.; Kim, H.; Tse, C.K. Adaptive active capacitor converter for improving stability of cascaded DC power supply system. *IEEE Trans. Power Electr.* **2012**, *28*, 1807–1816. [CrossRef]
34. Sartori, H.C.; Hey, H.L.; Pinheiro, J.R. An optimum design of PFC Boost Converters. *IEEE Trans. Power Electr.* **2009**, *13*, 1–8.
35. Coruh, N.; Urgun, S.; Erfidan, T. Design and implementation of flyback converter. In Proceedings of the IEEE Industrial Electronics and Applications, Taichung, Taiwan, 15–17 June 2010; pp. 1189–1193.
36. Sun, J.; Mitchell, D.M.; Greuel, M.F.; Krein, P.T.; Bass, R.M. Averaged modeling of PWM converters operating in discontinuous Conduction mode. *IEEE Trans. Power Electr.* **2001**, *16*, 482–492.
37. DigiKey Electronics. Available online: http://www.digikey.com (accessed on 26 June 2016).
38. Mouser Electronics. Available online: http://www.mouser.com (accessed on 26 June 2016).
39. Dropbox. Available online: https://www.dropbox.com/sh/imo3h8t51ozmoqf/AACBagr8j3zi9-M-SOHPBTeSa?dl=0 (accessed on 26 June 2016).
40. Jain, M.P.; Ray, L.M. Field pattern and associated losses in aluminum sheet in presence of strip bus bars. *IEEE Trans. Power Appar. Syst.* **1970**, *PAS-89*, 1525–1539. [CrossRef]
41. Hasaneen, B.M.; Mohammed, A.A.E. Design and simulation of DC-DC boost converter. In Proceedings of the IEEE Power System Conference, Aswan, Egypt, 12–15 March 2008; pp. 335–340.
42. El-Zanaty, M.; Orabi, M.; El-Sadek, M.Z. Review of synchronous buck converter design optimization. In Proceedings of the IEEE Power System Conference, Aswan, Egypt, 12–15 March 2008; pp. 588–592.